

# Modeling and Simulation of Atmospheric Synthetic Wind Field in Flight Simulation

Weiting Cui and Xiaoyong Lei

*State Key Laboratory of Virtual Reality Technology and Systems*

*Beihang University, Beijing, 100191 China*

cuiweiting@buaa.edu.cn

**Abstract**—As an important part of atmosphere, impact of wind field on the aircraft cannot be ignored in engineering and research. Four forms of wind model are modeled and simulated to describe the atmospheric synthetic wind field. To solve the problem of large amount of calculation existed in traditional generation method of three-dimensional atmospheric turbulence field, correlation function was introduced to generate atmospheric turbulence field of Von Karman spectrum.

According to the vortex core boundary conditions, a new damping factor was given to improve the vortex ring principle model's singular point in the vortex filament. These models of synthetic wind field were tested in one type of flight simulator and the results indicate these methods' effectiveness. These models can be used in flight simulation and the design of the flight simulator.

**Keywords**-Wind Field Model; Atmospheric Turbulence; Microburst; Flight Simulator

## I. INTRODUCTION

Flight simulator is an integrated simulation system on the ground for simulation of aircraft to perform various missions in a variety of conditions. It has been widely used in the design and development of the aviation industry, as well as the training of pilots and crewmembers in military aircrafts and civilian aircrafts. It is an important application of simulation technology and virtual reality technology in the aviation industry. As main manifestations of the atmosphere, Impact of variable wind field on aircraft performance cannot be ignored. Therefor the response of aircraft can be tested under different wind fields due to the establishment of an atmospheric synthetic wind field model, so as to further improve and enhance the performance of the aircraft.

Modeling of atmospheric synthetic wind field is a multidisciplinary problem. It requires not only the knowledge of hydrodynamics and aerodynamics, but also the understanding of virtual reality technology in certain depth. Wind field modeling technology has been researched in a certain extent in the past flight simulation, and mathematical models of some basic wind fields have been built. Most of these models are based on actual observations and built using fluid dynamics method. But these models are only fixed-form wind field models built according to the requirement of specific flight simulation, and it does not apply to the flexibility and

versatility requirement of any flight simulator in any condition. At the same time, the wind field model must be optimized so that meets both the system authenticity requirements and system real-time demand.

Under the above background conditions, the paper research into the modeling and simulation technology of atmospheric synthetic wind field, improve the modeling and simulation technology of some wind fields in current flight simulation, and integrate the atmospheric synthetic wind field model into the flight simulator so that meets the system authenticity and real-time requirements. It can provide better support for flight simulator, and make important significance for completing flight simulation model and promoting the development of virtual test technology.

## II. BASIC WIND FIELD TYPES AND CHARACTERISTICS

Wind is the movement of air in relation to the earth's surface, namely atmospheric motion. Atmospheric motion includes a variety of levels and temporal scales. Level scale range from zero meters to several thousand kilometers, and temporal scales range from seconds to years. In meteorology, atmospheric motions will usually be divided into large-scale, medium-scale and small-scale atmospheric motions of different scales. Large-scale atmospheric motions include atmospheric circulation, local circulation, etc. Mesoscale atmospheric motions include low-level wind shear, atmospheric turbulence, etc.

Large-scale atmospheric motion model is mainly used to understand quarterly changes and annual changes of wind in order to make better use of wind energy. In the virtual test vehicle, the small-scale wind field model is the main object of study. Considering the impact of wind in atmospheric environment on the aircraft flight characteristics, according to the decomposition of wind speed profiles<sup>[1]</sup>, the total wind speed is generally broken down into the average wind, atmospheric turbulence, wind shear and gust four forms. The following are introductions and analyses of characteristics of these several forms of wind.

### A. Average wind

The average wind is the reference value of the speed of the wind. It changes with time and space, and means the average wind speed within a specific time. The average wind changes

with time, such as the daily change, monthly change and quarterly change. The average wind changes with space, such as the average wind change with height. Generally the average wind speed changes between 0-10m/s, and increases with the increase of height, varies with the change of climate.

### B. Atmospheric turbulence

The atmosphere is always in the state of turbulent motion. The basic characteristic of the turbulent motion is the irregularity of velocity field moving along the spatial and temporal distribution. While wind appearing, it is often accompanied by turbulence. Turbulence in wind speed section line appears as the continuous random pulsation superimposed on the average wind. It also changes with time and space. We can say that the average wind speed is low-frequency part of wind speed and the turbulent wind speed is the high-frequency part of wind speed.

### C. Wind shear

Wind shear is the spatial variation of wind vector in a specific direction (horizontal or vertical direction). Low-level wind shear in accordance with the physical reasons for the formation can be divided into frontal wind shear, wind shear associated with the ground strong winds, and wind shear associated with the convective storms, etc. In the latter of which, which the outflow range is less than 4km, called the microburst, and it greatest harms to flight. Therefore, this paper mainly researches the microburst.<sup>[2]</sup> Due to the air convection the updraft generates, which send the warm and humid air with strong buoyancy to the position of high altitude. As the altitude increases, the air cools down and liquefies. Then the increased process stops. At this time, after cooling the air density increases, and it begin to rapidly sink to the ground, generating wind shear in the vertical direction. After this downburst impact the ground within a limited near-Earth space area, it diverges to the sides from the circle center of the point of impact, steers and becomes the horizontal wind shear parallel to the ground.

### D. Gust

The gust also has the characteristic that it has a velocity field along with a spatial and temporal distribution of irregularities. Compared with the turbulence, turbulence is a continuous random variation of wind farm, while the gust is a discrete or certain change. The gust has the characteristics of suddenness and intenseness. It harms to flight simulator greatly. In engineering applications, the gust can be characterized by discrete wind shear, peak of the turbulence in the atmosphere, flow of aircraft wake region, etc.

## III. MODELING AND SIMULATION OF THE ATMOSPHERIC SYNTHETIC WIND FIELD

### A. Modeling and simulation of the average wind field

#### a) Average wind field model

In a flight simulator, you can usually do not consider the average wind changes with time, that so-called "frozen field"

hypothesis<sup>[3]</sup>. The average wind changes with height can be described by the law of logarithm distribution. In (1):

$$V_a = \frac{V_{a0}}{k} \ln \frac{H}{H_0} \quad (1)$$

Where  $H_0$  is the surface roughness height (m), about 1/30-1/10 of the ground height; k is Karman constant, dimensionless, k=0.4;  $V_{a0}$  is called friction velocity(m/s), which depends on the shear stress on the ground and the air density.

#### b) Simulation of the average wind field

According to the analysis of average speed data from amount of wind field, take  $H_0 = 3m$ , k=0.4,  $V_{a0} = 0.4m/s$ . The average wind speed at the height of 10-10000m is shown in Fig.1.

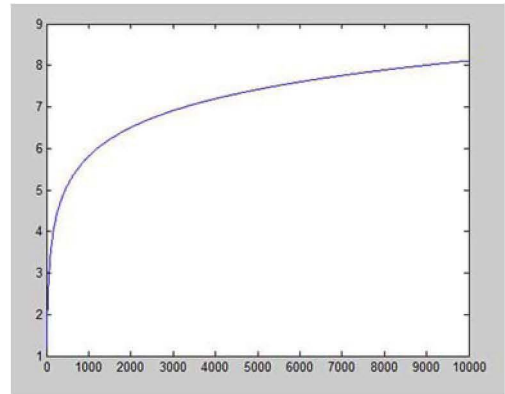


Figure 1. Variation of the average wind speed with height

### B. Modeling and simulation of the atmospheric turbulence wind field

The current three-dimensional atmospheric turbulence simulation method has many common problems such as large amount of calculation, serious computer memory, poor real-time simulation, etc. It cannot meet the needs of real-time flight simulator. The atmospheric turbulence simulation method based on the correlation function uses recursive model to generate atmospheric turbulence data with the characteristics of small amount of calculation and small computer memory. It can be performed in real-time simulation.<sup>[4]</sup> This paper intends to research on and build the stochastic process model of three-dimensional atmospheric turbulence field based on correlation functions, and generate the three-dimensional atmospheric turbulence field.

#### a) The basic principle of the numerical simulation of atmospheric turbulence

The basic principle of the numerical simulation of turbulence is the general principle of stochastic processes generated. By using the shaping filter obtained, white noise shaping is converted to colored noise and output. The principle is shown in Fig.2. Where white noise signal uses the Gaussian distribution of pseudo-random sequence with a mean of 0 and standard deviation of 1. The key is the determination of transfer function G(s).



Figure 2. Numerical simulation principle of the atmospheric turbulence

In the control process, the links that can convert white noise into colored noise is called shaping filter.<sup>[5]</sup> Spectrum of white noise is a constant value. Make it as a unit value. By a filter with the transfer function of  $G(s)$ , the unit of white noise  $r(t)$  generates the random process  $u(t)$ . The spectral function of  $u(t)$  is:

$$\Phi(\omega) = G^*(i\omega)G(i\omega) = |G(i\omega)|^2 \quad (2)$$

where \* denotes the complex conjugate. This method is also often used in projects to simulate stationary random process.

When the time spectrum function can be decomposed as above, the parameters of the filter can be shaped, so that we can simulate in the time domain.<sup>[6]</sup> By decomposing the time spectrum function of the turbulence according to (2) decomposition, we can get the transfer function  $G(s)$  of the shaping filter which the given spectrum need.

### b) Correlation function and spectrum function of atmospheric turbulence

For the correlation function and spectrum of atmospheric turbulence in flight simulation, H.L.Dryden<sup>[7]</sup> and T.Von Karman make the statistics and derivation according to different theoretical system based on measured data respectively. H.L.Dryden gives the longitudinal and transverse correlation function of atmospheric turbulence first, and then derives the spectrum function. T. Von Karman gives the energy spectrum of atmospheric turbulence first, as shown in (3), and then derives the spectrum and related functions of the three turbulent components, as shown in (4)-(6).

$$E(\Omega) = \sigma^2 \frac{55L}{9\pi} \frac{(aL\Omega)^4}{[1+(aL\Omega)^2]^{17/6}} \quad (3)$$

$$\left. \begin{aligned} \Phi_{uu}(\Omega) &= \sigma_u^2 \frac{L_u}{\pi} \frac{1}{[1+(aL_u\Omega)^2]^{5/6}} \\ \Phi_{vv}(\Omega) &= \sigma_v^2 \frac{L_v}{\pi} \frac{1+(8/3)(2aL_v\Omega)^2}{[1+4(aL_v\Omega)^2]^{11/6}} \\ \Phi_{ww}(\Omega) &= \sigma_w^2 \frac{L_w}{\pi} \frac{1+(8/3)(2aL_w\Omega)^2}{[1+4(aL_w\Omega)^2]^{11/6}} \end{aligned} \right\} \quad (4)$$

$$f(\xi) = \frac{2^{2/3}}{\Gamma(1/3)} \xi^{1/3} K_{1/3}(\zeta) \quad (5)$$

$$g(\xi) = \frac{2^{2/3}}{\Gamma(1/3)} \xi^{1/3} [K_{1/3}(\zeta) - \frac{1}{2} \zeta K_{2/3}(\zeta)] \quad (6)$$

Where  $\zeta = \xi/(aL)$ ,  $a=1.339$ ,  $\Gamma$  is Gamma function,  $K$  is Bessel function.

Dryden spectrum model and Von Karman spectrum model are not very different in the low band. Von Karman spectrum model will be more accurate when in high band. However, due to the spectrum function of Von Karman model cannot be decomposed conjugate, and the spectrum function of Dryden model is a rational expression which can be used for factoring, so that the simulation can be realized in the time domain. Therefore, previous studies often make conjugate decomposition to the Dryden model in order to generate the atmospheric turbulence.

In this paper, in order to improve the fidelity of the flight dynamics system simulation, the proposed method in literature is intended to be used.<sup>[8]</sup> We change the past modeling method based on Dryden model, and make rationalized processing to the Von Karman model that cannot be directly used for simulation, directly come up with a simplified model of Von Karman model approach to the Von Karman model, thus realize to a three-dimensional numerical simulation of Von Karman turbulence model.

- c) Numerical simulation of three-dimensional atmospheric turbulence based on Von Karman model.
- 1) The determination of shaping filter parameters

In order to make the model can be simulating achieved in the time domain simulation, we make rationalized approach to the Von Karman model, and reduced to first-order, then get:

$$\left. \begin{aligned} G_u(s) &= \frac{K_u}{T_u s + 1} \\ K_u &= \sigma_u \sqrt{\frac{L_u}{\pi V}}, T_u = \left( \frac{a L_u}{V} \right)^{5/6} \end{aligned} \right\} \quad (7)$$

$$\left. \begin{aligned} G_v(s) &= \frac{K_v}{T_v s + 1} \\ K_v &= \sigma_v \sqrt{\frac{L_v}{\pi V}}, T_v = \sqrt{\frac{3}{8}} \left( \frac{2 a L_v}{V} \right)^{5/6} \end{aligned} \right\} \quad (8)$$

$$\left. \begin{aligned} G_w(s) &= \frac{K_w}{T_w s + 1} \\ K_w &= \sigma_w \sqrt{\frac{L_w}{\pi V}}, T_w = \sqrt{\frac{3}{8}} \left( \frac{2 a L_w}{V} \right)^{5/6} \end{aligned} \right\} \quad (9)$$

- 2) The generation of atmospheric turbulence signal sequence

Make the filter transfer function:

$$G(s) = \frac{x(s)}{r(s)} = \frac{c}{s+a} \quad (10)$$

After derivation, to obtain difference equations used for the simulation:

$$x_{i+1} = e^{-aT} x_i + \frac{c}{a} (1 - e^{-aT}) r_i \quad (11)$$

Where  $T$  is the sampling period, that the time step  $r(s)$  is the input of the Laplace transform form of the pseudo-random number.  $a = 1/T$ ,  $c = K/T$ . Thus we constantly generate the required atmospheric turbulence sequence according to (11).

### 3) Simulation results

According to the derivation, take  $L_w = 70m$ ,  $\Delta x = 10m$ ,  $V = 80m/s$ ,  $\sigma_w = 3.5$ , the speed fragment of turbulence in the vertical direction was obtained, shown in Fig. 3.

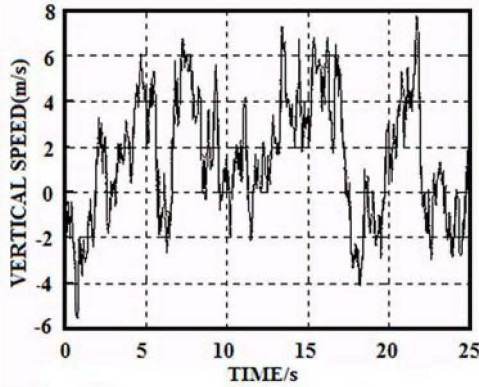


Figure 3. Speed fragment of turbulence in the vertical direction

## C. Modeling and simulation of the Microburst wind field

### a) Modeling of Microburst wind field

According to the Microburst wind shear model needs of Flight Simulator, a three-dimensional space model based on vortex ring theory will be built on the proposed in this paper. Through in-depth improvements to the vortex ring modeling method, make it more consistent with the actual wind field. Vortex ring principle model of the Microburst was first proposed by Woodfield and Woo.<sup>[9]</sup> In this model, the induced velocity field of vortex ring is used to simulate Microburst field. Since the wind speed in the vertical component of the ground is 0, by symmetrically arranging two vortex rings which strength is  $\Gamma$  at the same distance from the ground level height, thus satisfy the boundary conditions. Among them, the vortex ring above the ground is called the primary vortex ring, the vortex ring which is symmetric called image vortex ring, the center of the vortex ring is called a vortex filament. <sup>[10]</sup> The vortex ring model is shown in Fig.4.

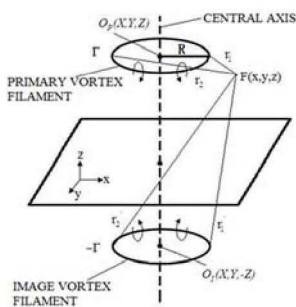


Figure 4. The model based on vortex ring theory

In Fig.4,  $O_{xyz}$  is the ground coordinate,  $x$ -axis pointing north,  $y$ -axis pointing east,  $z$ -axis vertically upwards, Origin can be selected in the position that both high latitude and longitude are 0. The center coordinates of primary vortex ring are  $O_p(X,Y,Z)$ , the center coordinates of the image vortex ring are  $O_i(X,Y,-Z)$ .  $F$  is the reference particle, its coordinates are  $(x, y, z)$ , The radius of vortex ring is  $R$ .

Expression of vortex circulation line equation:

$$\psi = \frac{\Gamma}{2\pi}(r_1 + r_2)[F(\lambda) - E(\lambda)] \quad (12)$$

Where  $\Gamma$  is strength of the vortex ring,  $r$  is the distance from reference particle to vortex ring axis. The minimum distance from reference particle to vortex filament of the primary vortex ring is  $r_1$ , the maximum distance is  $r_2$ .  $F(\lambda)$  and  $E(\lambda)$  are elliptic integral functions. The formula can be used to approach when calculating Elliptic integrals:

$$F(\lambda) - E(\lambda) \approx \frac{0.788\lambda^2}{0.25 + 0.75\sqrt{1-\lambda^2}} \quad (13)$$

$$\text{Where } \lambda = \frac{r_2 - r_1}{r_2 + r_1}$$

The streamline equation of primary vortex ring is:

$$\psi_p = -\frac{\Gamma}{2\pi} \cdot \frac{0.788\lambda_p^2(r_1 + r_2)}{0.25 + 0.75\sqrt{1-\lambda_p^2}} \quad (14)$$

Since the primary vortex ring and image vortex ring is symmetric to the level of the ground, we can get the streamline equation of image vortex ring. The whole streamline equation is the superposition of them:

$$\psi_\Sigma = \psi_p + \psi_i \quad (15)$$

The velocity field of single vortex ring Microburst model can be calculated by following induced formula:

$$\left. \begin{aligned} V_x &= \left( \frac{x - X}{r^2} \right) \frac{\partial \psi_\Sigma}{\partial z} \\ V_y &= \left( \frac{y - Y}{r^2} \right) \frac{\partial \psi_\Sigma}{\partial z} \\ V_z &= \left( -\frac{1}{r} \right) \frac{\partial \psi_\Sigma}{\partial r} \end{aligned} \right\} \quad (16)$$

### b) Calculation of induced velocity in the central axis of the vortex ring

In the central axis of the vortex ring, since  $r=0$ , Field speed of the Microburst cannot be directly calculated by (16) and need to be improved. By the method of striking limit, we can eliminate the problem of speed singularity that infinitely close to the central axis in the method of vortex ring. (17), (18) give the limit speed equation at the vortex ring axis.

$$V_x = V_y = 0 \quad (17)$$

$$V_z = \frac{\Gamma R^2}{2} \{ [R^2 + (z+Z)^2]^{1/2} - [R^2 + (z-Z)^2]^{1/2} \} \quad (18)$$

### c) Calculation of induced velocity within the vortex core

Fig.5 describes the changes of vertical wind in flight path of the Microburst field built by vortex principle model when the aircraft flight level crossing vortex filament. From the figure we can see that, the position of vortex filament is a singular point of the wind speed values. On the inside of the vortex filament, wind speed is  $-\infty$ , on the outside of the vortex filaments, wind speed is  $+\infty$ . This is inconsistent with the Microburst wind field situation. Multiply the respective formulas in (16) by a damping factor, and make the wind speed inside the vortex core decay to 0 at the vortex filament, while the wind speed does not change outside the vortex core.<sup>[11]</sup> After the introduction of the damping factor, the changes of vertical wind in flight path of the microburst field when the aircraft flight level crossing vortex filament are shown in Fig.6.

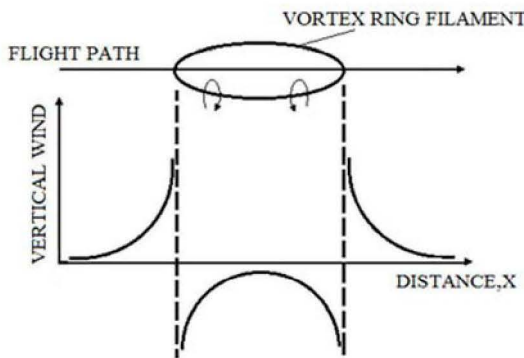


Figure 5. The singularity of wind speed at the vortex filament

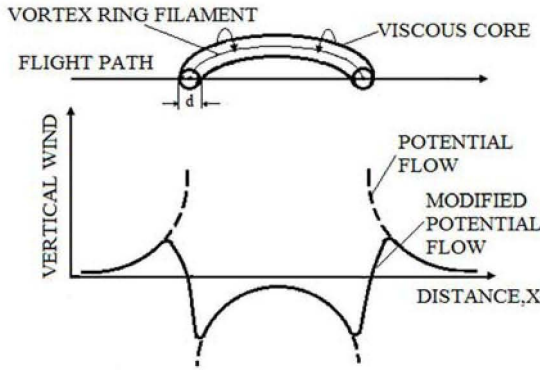


Figure 6. Viscous vortex core modification of a vortex ring

Generally, the form of the damping factor is given by the experience. At present, there are two forms of the damping factor more commonly used, shown in (19) and (20):

$$\zeta = 1 - \exp\left\{-\frac{\left(\frac{r_1}{R}\right)^2}{[0.4215\frac{d}{R} + 0.0822\left(\frac{d}{R}\right)^2 - 0.0969\left(\frac{d}{R}\right)^3]^2}\right\} \quad (19)$$

$$\zeta = 1 - \exp\left\{-\left(\frac{r_1}{d/2}\right)^2\right\} \quad (20)$$

We can see that there is a large amount of calculation in (19), and it is not suitable for real-time simulation systems. In (20), for any point F at the vortex core boundary, the minimum distance to the vortex filament is  $r_1 = d/2$ , taken into the (20) gets that  $\zeta = 1 - e^{-1} = 0.6321$ . There is a big gap between damping factor  $\zeta$  at the boundary of the vortex core and 1, shows that it does not stop attenuating the vortex core boundary. Attenuation to the speed of Microburst field is still conducted in some areas outside the vortex core. Velocity distribution on the region of the vortex ring principle model is too large. This paper makes the following improvements:

$$\zeta = 1 - \exp\left[-\left(\frac{K \cdot r_1}{d/2}\right)^2\right] \quad (21)$$

Value of the coefficient K is determined by vortex core boundary conditions. When  $K=4$ , where  $r=d/2$  at the vortex core boundary,  $\zeta = 1 - e^{-16} = 0.99999989$ , close enough to 1, thus  $K=4$  is consistent with the vortex core boundary conditions. Then:

$$\zeta = 1 - \exp\left[-\left(\frac{4r_1}{d/2}\right)^2\right] \quad (22)$$

### d) Stimulation of the Microburst wind field

Based on the above derivation, set the basic parameters of the model: primary vortex ring center coordinates  $O_p(0, 0, 800)$ , vortex ring radius  $R=1500m$ , vortex ring strength  $\Gamma = 30000m^2/s$ , vortex core radius  $d/2=500m$ . Fig.7 is the wind velocity vector graph generated at the center axis of the vortex ring and section of the axis y containing the horizontal and vertical directions. As can be seen from the figure, the velocity field induced by vortex ring principle model has the basic characteristics of Microburst field, can effectively simulate the downdrafts and outflow velocity changes of the Microburst.

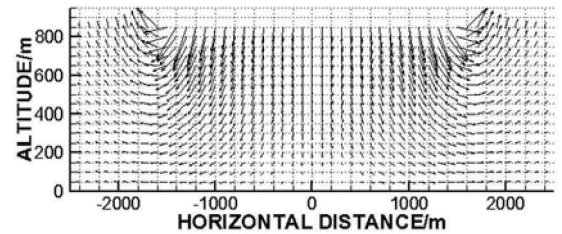


Figure 7. Velocity vector graph at the center axis of the vortex ring

### D. Gust wind field model.

#### a) Modeling of the gust wind field

According to the profile geometry of the gust model<sup>[12]</sup>, the gust model can be divided into rectangular, trapezoidal, triangular, sinusoidal and "1-consine" shape, etc. In Engineering, the full wavelength "1-consine" and the half-wavelength "1-consine" gust model are usually used to describe.

The full wavelength "1-consine" model:

$$V_g = \begin{cases} 0 & h < 0 \\ \frac{V_{g\max}}{2} \left(1 - \cos \frac{\pi h}{d_m}\right) & 0 \leq h \leq 2d_m \\ 0 & h > 2d_m \end{cases} \quad (23)$$

The half-wavelength "1-consine" model:

$$V_g = \begin{cases} 0 & h < 0 \\ \frac{V_{g\max}}{2} \left(1 - \cos \frac{\pi h}{d_m}\right) & 0 \leq h \leq d_m \\ 0 & h > d_m \end{cases} \quad (24)$$

Where  $V_g$  is the gust speed corresponding to the height  $h$ ,  $V_{g\max}$  is the amplitude of the gust,  $d_m$  is the half thickness of the gust layer, its size is taken to be some 25 to 150m or  $(2 \sim 3 V_{g\max})$ .

### b) Stimulation of the gust wind field model

The gust model above can be used to characterize the gust component in either direction. Compared with the full wavelength "1-consine" discrete gust model, the half-wavelength "1-consine" discrete gust model is more flexible and convenient to use. For example, With more than one half-wavelength of "1-consine" discrete gust models sequentially connected, a new gust mode can be formed. Therefore, this paper adopts the half-wavelength "1-consine" discrete gust model to model.

Take  $d_m = 85m$ ,  $V_{g\max} = 30m/s$ , get the variation relationship of the gust wind speed value given position and direction with the height, as shown in Fig.8.

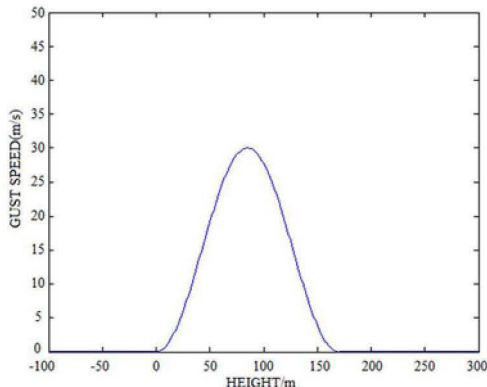


Figure 8. Variation relationship of the gust wind speed with height

## IV. APPLICATION OF THE ATMOSPHERIC WIND FIELD MODEL IN FLIGHT SIMULATOR

Atmospheric motion is the main disturbance source of aircraft flight path and flight attitude. Therefore, the establishment of a synthetic atmospheric wind field environment model in the flight simulator is of great significance. This paper uses the FlightGear platform as the running support platform, takes the virtual aircraft models as

test subjects, and simulates responses of full mission flight simulator under the actions of various synthetic wind fields. Provide an important reference for the design of flight simulation system and flight simulator.

Through the IOS simulation interface, the user can set the parameter information of various types of basic wind fields in the master control interface. The above information pass through the interface to a synthetic wind field model, the wind velocity vector value of the current particle will be calculated in each step of the real-time simulation, and the value will be passed to the dynamics model of the aircraft ontology to calculate. Assuming the plane open automatic driving, changes in airspeed, vertical speed and pitching angle were shown in Fig.9-Fig.10 when it encounters microburst or not during landing. In addition, the plane passes the center axis of the vortex ring at 912 frames. Changes in airspeed when the plane encounters atmospheric turbulence are in Fig.11.

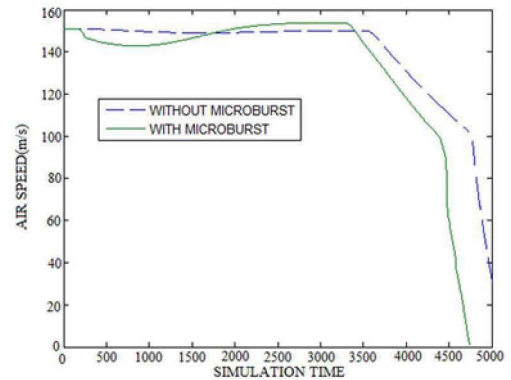


Figure 9. Changes in airspeed when the plane encounters microburst during landing

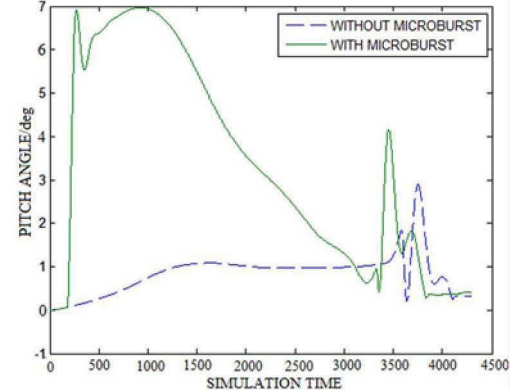


Figure 10. Changes in pitch angle when the plane encounters microburst during landing

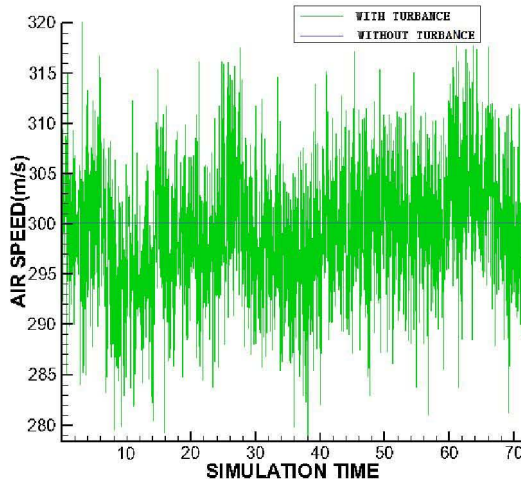


Figure 11. Changes in airspeed when the plane encounters atmospheric turbulence

## V. CONCLUSIONS

In this paper, starting from the actual engineering, for the purpose of enhance simulation fidelity of the flight simulator, we used engineering simplified model to describe the main features of the atmospheric synthetic wind field and improve part of the model, determined atmospheric wind field model, and made the flight dynamics simulation in flight simulator. We got following conclusions.

- 1) Used the method of correlation function to generate atmospheric turbulence field of Von Karman spectrum, made rationalized processing to the Von Karman mode, made it be simulating implemented in the time domain simulation. Solved the problem that Dryden model has poor accuracy at high frequencies and the problem that large amount of calculation existed in traditional generation method of three-dimensional atmospheric turbulence wind field.
- 2) Researched on the modeling techniques of the microburst wind shear, selected the method of vortex ring principle to build three-dimensional Microburst field. By introducing new damping factor, solved the problem that vortex ring principle model has a singular point in the vortex filament.
- 3) Built the atmospheric synthetic wind field constituted of average wind field, atmospheric turbulence wind field, wind shear wind field and gust wind field. Through flexible setting of wind field model parameters, all kinds of complex synthetic wind fields can be simulated, and the needs of adapting to different virtual flight simulator tests can be met.

4) Applied the Synthetic atmospheric wind field model to the flight simulator, used the FlightGear platform as the running support platform, took the virtual aircraft models as test subjects, simulated responses of full mission flight simulator under the actions of various synthetic wind fields. Provided an important reference for the design of flight simulation system and flight simulator.

In future, based on the consideration of practicability and improving system simulation fidelity of the flight simulator, author will research on the modeling of the mountain disturbance wind field, storm field, frontal wind shear, etc. to build a more comprehensive wind field model, in order to improve the flight simulator environment simulation system.

## ACKNOWLEDGMENT

This work is supported by the Fundamental Research Funds for the Central Universities: YWF-13-D2-HK-26; and Beijing Municipal Science and Technology Plan: Z111100074811001. We thank anonymous reviewers for their valuable comments.

## REFERENCES

- [1] D. X. He. Wind Engineering and Aerodynamics[M]. National Defence Industry Press, 2006.
- [2] Chay M T, Letchford C W. Pressure distributions on a cube in a simulated thunderstorm downburst—Part A: stationary downburst observations[J]. Journal of wind engineering and industrial Aerodynamics, 2002, 90(7): 711-732.
- [3] W. L. Wang. Atmospheric Wind Field Modeling and its Application [D]. National University of Defense Technology, 2009.
- [4] G. Liu, X. R. Wang, and R. Z. Jia. Engineering Simulation Method of Variable Wind Field in Synthetic Natural Environment [J]. Journal of System Simulation, 2006:297-300.
- [5] Y. Wu. Research on Modeling and Application Technologies of Wind Field in Virtual Test[D]. Harbin Institute of Technology, 2011.
- [6] Morelli E A, Cunningham K. Aircraft Dynamic Modeling in Turbulence[C]//AIAA Atmospheric Flight Mechanics Conference. 2012.
- [7] G. X. Hong, Y. L. Xiao. MONTE CARLO Simulationfor 3-D - FieldofAtmosphericTurbulence[J]. ActaAeronauticaetAstronauticaSinica. 2001,22(6):542-545.
- [8] F. Zhang, P. Wang, C. Wang. Simulation of Three -Dimensional Atmospheric Turbulence Based onVon Karman Model[J]. Computer Simulation, 2007, 124(1):35-38.
- [9] Woodfield A A, Woods J F. Worldwide experience of wind shear during 1981-1982[R]. ROYAL AIRCRAFT ESTABLISHMENT BEDFORD (ENGLAND), 1983.
- [10] Z. X. Gao, H. B. Gu. Research on Modeling of Microburst for Real Time Flight Simulation [J]. Journal of System Simulation, 2008, 20(33): 6524-6534.
- [11] Zhao Yiyuan, A.E. Bryson. A Simplified Ring-Vortex Downburst Model[C]. 28th Aerospace Sciences Meeting, 1990: 1~11.
- [12] Xiao Yelun, JinChangjiang. Flight principles in atmospheric disturbance [M]. Beijing: National Defence Industry Press, 1991.